



AIAA 2003–3498

**Viscous Aerodynamic Shape
Optimization of Wings including
Planform Variables**

Kasidit Leoviriyakit, Sangho Kim, and Antony Jameson
Stanford University, Stanford, CA 94305-4035

21st Applied Aerodynamics Conference
Orlando, Florida/June 23–26, 2003

VISCOUS AERODYNAMIC SHAPE OPTIMIZATION OF WINGS INCLUDING PLANFORM VARIABLES

Kasidit Leoviriyakit, * Sangho Kim, † and Antony Jameson ‡
Stanford University, Stanford, CA 94305-4035

During the last decade, aerodynamic shape optimization methods based on control theory have been intensively developed. The methods have proved to be very effective for improving wing section shapes for fixed wing-planforms. Building on this success, extension of the control theory approach to variable planforms has yielded further improvement. This paper describes the formulation of planform optimization techniques based on control theory for aerodynamic shape design in viscous compressible flow modeled by the Navier-Stokes equations. It extends the previous work on wing planform optimization based on inviscid calculations, providing increased realism, and alleviating shocks that would otherwise form in the viscous solution over the final inviscid design. In order to realize a meaningful design, the structural weight, estimated by a statistical weight model, is taken into account. A practical method to combine the structural weight into the design cost function is studied. An extension of a single to a multiple objective cost function is also considered. Results of optimizing a wing-fuselage of a commercial transport aircraft show a successful trade-off between the aerodynamic and structural cost functions, leading to improved wing planform designs. The results also support the necessity of including the structural weight in the cost function. Furthermore, by varying the weighting constant in the cost function, a Pareto front is captured, broadening the design range of optimal shapes.

INTRODUCTION

CFD has played a key role in the aerodynamic design process. However, it has generally not been used as a direct design tool, but as an aid to analyze the fluid flow. The design process has still been done by trial and error based on the intuition and experience of the designer. In the 1970s several efforts were made to exploit CFD as a direct design tool,¹⁻⁴ and since then the focus of CFD applications has shifted to aerodynamic design.⁵⁻¹¹ This shift has been mainly motivated by the availability of high performance computing platforms and by the development of new and efficient analysis and design algorithms. In particular, automatic design procedures which use CFD combined with gradient-based optimization techniques have had a significant impact by removing difficulties in the decision making process faced by the aerodynamicist.

In gradient-based optimization techniques, a control function to be optimized (an airfoil shape, for example) is parameterized with a set of design variables, and a suitable cost function to be minimized or maximized is defined (drag coefficient, lift/drag ratio, difference from a specified pressure distribution, etc). Then, a constraint, the governing equations in the present study, can be introduced in order to ex-

press the dependence between the cost function and the control function. The sensitivity derivatives of the cost function with respect to the design variables are calculated in order to get a direction of improvement. Finally, a step is taken in this direction, and the procedure is repeated until convergence to a minimum or maximum is achieved.

In high-dimensional parameterization optimizations such as aerodynamic shape optimization, gradient calculation can be the most time consuming portion of the design process. Therefore, it is essential to find a fast and accurate methods to calculate the gradient.

Gradient information can be computed using a variety of approaches such as the finite-difference method, the complex step method,¹² and automatic differentiation.¹³ Unfortunately, their computational cost is still proportional to the number of design variables in the problem. An alternative choice is to treat the design problem as a control problem. This approach has dramatic computational cost advantages when compared to any of the other methods. The foundations of control theory for systems governed by partial differential equations were laid by J.L. Lions.¹⁴

The control-theory approach is often called the adjoint method, since the necessary gradients are obtained via the solution of the adjoint equations of the governing equations of interest. The adjoint method is extremely efficient since the computational expense incurred in the calculation of the complete gradient is effectively *independent* of the number of design variables. The only cost involved is the calculation of *one* flow solution and *one* adjoint solution whose complexity is similar to that of the flow solution. Control theory was

*Doctoral Candidate, AIAA Member

†Postdoctoral Fellow, AIAA Member

‡Thomas V. Jones Professor of Engineering, Department of Aeronautics and Astronautics, AIAA Member

Copyright © 2003 by the American Institute of Aeronautics and Astronautics, Inc. No copyright is asserted in the United States under Title 17, U.S. Code. The U.S. Government has a royalty-free license to exercise all rights under the copyright claimed herein for Governmental Purposes. All other rights are reserved by the copyright owner.

applied in this way to shape design for elliptic equations by Pironneau¹⁵ and it was first used in transonic flow by Jameson.^{6,7,16} Since then this method has become a popular choice for design problems involving fluid flow.^{9,17-19} During the last decade, the methods have been intensively developed and have been proved to be very effective for improving wing section shapes for fixed wing-planforms.^{20,21}

Wing planform modifications have the potential to yield significantly larger improvements in wing performance, but can also adversely affect both wing weight and stability and control characteristics. It is well known that the induced drag varies inversely with the square of the span. Hence the induced drag can be reduced by increasing the span. Moreover, shock drag in transonic flow might be reduced by increasing sweep-back or increasing the chord to reduce the thickness to chord ratio. Consequently, a pure aerodynamic optimization may lead to highly suspect results because the decrease in drag might come at the expense of the increase in wing weight. Therefore it is essential to account for the effect of planform change on wing weight, and for practical design purposes, a fast and accurate method to predict the wing weight and its gradient is necessary.

In this work, we report improvements in a design for wing planform optimization²² and its extension to include viscous effects. While inviscid calculations have proven useful for the design of transonic wings at the cruise condition, the required changes in the section shape are comparable in magnitude to the displacement thickness of the boundary layer. Thus viscous design provides increased realism, and alleviates shocks that would otherwise form in the viscous solution over the final inviscid design. Accurate resolution of viscous effects such as separation and shock/boundary layer interaction is also essential for optimal design encompassing off-design conditions.

MATHEMATICAL FORMULATION

Design using the Navier-Stokes Equations

The application of control theory to aerodynamic design problems is illustrated in this section for the case of three-dimensional wing design using the compressible Navier-Stokes equations as the mathematical model. It proves convenient to denote the Cartesian coordinates and velocity components by x_1, x_2, x_3 and u_1, u_2, u_3 , and to use the convention that summation over $i = 1$ to 3 is implied by a repeated index i . Then, the three-dimensional Navier-Stokes equations may be written as

$$\frac{\partial w}{\partial t} + \frac{\partial f_i}{\partial x_i} = \frac{\partial f_{vi}}{\partial x_i} \quad \text{in } \mathcal{D}, \quad (1)$$

where the state vector w , inviscid flux vector f and viscous flux vector f_v are described respectively by

$$w = \begin{Bmatrix} \rho \\ \rho u_1 \\ \rho u_2 \\ \rho u_3 \\ \rho E \end{Bmatrix}, \quad f_i = \begin{Bmatrix} \rho u_i \\ \rho u_i u_1 + p \delta_{i1} \\ \rho u_i u_2 + p \delta_{i2} \\ \rho u_i u_3 + p \delta_{i3} \\ \rho u_i H \end{Bmatrix}, \quad (2)$$

$$f_{vi} = \begin{Bmatrix} 0 \\ \sigma_{ij} \delta_{j1} \\ \sigma_{ij} \delta_{j2} \\ \sigma_{ij} \delta_{j3} \\ u_j \sigma_{ij} + k \frac{\partial T}{\partial x_i} \end{Bmatrix}, \quad (2)$$

and δ_{ij} is the Kronecker delta function. Also,

$$p = (\gamma - 1) \rho \left\{ E - \frac{1}{2} u_i u_i \right\}, \quad (3)$$

and

$$\rho H = \rho E + p \quad (4)$$

where γ is the ratio of the specific heats. The viscous stresses may be written as

$$\sigma_{ij} = \mu \left(\frac{\partial u_i}{\partial x_j} + \frac{\partial u_j}{\partial x_i} \right) + \lambda \delta_{ij} \frac{\partial u_k}{\partial x_k}, \quad (5)$$

where μ and λ are the first and second coefficients of viscosity. The coefficient of thermal conductivity and the temperature are computed as

$$k = \frac{c_p \mu}{Pr}, \quad T = \frac{p}{R\rho}, \quad (6)$$

where Pr is the Prandtl number, c_p is the specific heat at constant pressure, and R is the gas constant.

Using a transformation to a fixed computational domain, the Navier-Stokes equations can be written in the transformed coordinates as

$$\frac{\partial (Jw)}{\partial t} + \frac{\partial (F_i - F_{vi})}{\partial \xi_i} = 0 \quad \text{in } \mathcal{D}, \quad (7)$$

where the inviscid terms have the form

$$\frac{\partial F_i}{\partial \xi_i} = \frac{\partial}{\partial \xi_i} (S_{ij} f_j),$$

the viscous terms have the form

$$\frac{\partial F_{vi}}{\partial \xi_i} = \frac{\partial}{\partial \xi_i} (S_{ij} f_{vj}),$$

and S_{ij} are the coefficients of the Jacobian matrix of the transformation.

The geometry changes are represented by changes δS_{ij} in the metric coefficients. Suppose one wishes to minimize the cost function of a boundary integral

$$I = \int_{\mathcal{B}} \mathcal{M}(w, S) d\mathcal{B}_\xi + \int_{\mathcal{B}} \mathcal{N}(S) d\mathcal{B}_\xi$$

where $\mathcal{M}(w, S)$ could be an aerodynamic cost function, e.g. drag coefficient, and $\mathcal{N}(S)$ could be a structural cost function, e.g. wing weight. In the steady state flow, one can augment the cost function through Lagrange multiplier ψ as

$$I = \int_{\mathcal{B}} \mathcal{M}(w, S) d\mathcal{B}_\xi + \int_{\mathcal{D}} \psi^T \mathcal{R}(w, S) d\mathcal{D}_\xi + \int_{\mathcal{B}} \mathcal{N}(S) d\mathcal{B}_\xi,$$

where $\mathcal{R} = \frac{\partial(F_i - F_{vi})}{\partial \xi_i}$. A shape variation δS causes a variation

$$\delta I = \int_{\mathcal{B}} \delta \mathcal{M} d\mathcal{B}_\xi + \int_{\mathcal{D}} \psi^T \frac{\partial}{\partial \xi_i} \delta(F_i - F_{vi}) d\mathcal{D}_\xi + \int_{\mathcal{B}} \delta \mathcal{N} d\mathcal{B}_\xi$$

The second term on the RHS can be integrated by parts to give

$$\int_{\mathcal{B}} n_i \psi^T \delta(F_i - F_{vi}) d\mathcal{B}_\xi - \int_{\mathcal{D}} \frac{\partial \psi^T}{\partial \xi_i} \delta(F_i - F_{vi}) d\mathcal{D}_\xi. \quad (8)$$

and choosing ψ to satisfy the adjoint equation with appropriate boundary conditions depending on the cost function, the explicit dependence on δw is eliminated allowing the cost variations to be expressed in terms of δS and the adjoint solution, and hence finally in terms of the change $\delta \mathcal{F}$ in a function $\mathcal{F}(\xi)$ defining the shape.

Thus one obtains

$$\delta I = \int \mathcal{G} \delta \mathcal{F} d\xi = \langle \mathcal{G}, \delta \mathcal{F} \rangle$$

where \mathcal{G} is the infinite dimensional gradient (Frechet derivative) at the cost of one flow and one adjoint solution. Then one can make an improvement by setting

$$\delta \mathcal{F} = -\lambda \mathcal{G}$$

In fact the gradient \mathcal{G} is generally of a lower smoothness class than the shape \mathcal{F} . Hence it is important to restore the smoothness. This may be affected by passing to a Sobolev inner product of the form

$$\langle u, v \rangle = \int (uv + \epsilon \frac{\partial u}{\partial \xi} \frac{\partial v}{\partial \xi}) d\xi$$

This is equivalent to replacing \mathcal{G} by $\bar{\mathcal{G}}$, where in one dimension

$$\bar{\mathcal{G}} - \frac{\partial}{\partial \xi} \epsilon \frac{\partial \mathcal{G}}{\partial \xi} = \mathcal{G}, \quad \bar{\mathcal{G}} = \text{zero at end points}$$

and making a shape change $\delta \mathcal{F} = -\lambda \bar{\mathcal{G}}$.

Euler Adjoint Equations and Boundary Condition

In order to derive the adjoint equation in detail, (8) can be expanded as

$$\int_{\mathcal{B}} \psi^T (\delta S_{2j} f_j + S_{2j} \delta f_j) d\mathcal{B}_\xi$$

$$\begin{aligned} & - \int_{\mathcal{D}} \frac{\partial \psi^T}{\partial \xi_i} (\delta S_{ij} f_j + S_{ij} \delta f_j) d\mathcal{D}_\xi \\ & - \int_{\mathcal{B}} \psi^T (\delta S_{2j} f_{vj} + S_{2j} \delta f_{vj}) d\mathcal{B}_\xi \\ & + \int_{\mathcal{D}} \frac{\partial \psi^T}{\partial \xi_i} (\delta S_{ij} f_{vj} + S_{ij} \delta f_{vj}) d\mathcal{D}_\xi. \end{aligned} \quad (9)$$

It is convenient to assume that the shape modification is restricted to the coordinate surface $\xi_2 = 0$ so that $n_1 = n_3 = 0$, and $n_2 = 1$. Furthermore, it is assumed that the boundary contributions at the far field may either be neglected or else eliminated by a proper choice of boundary conditions as previously shown for the inviscid case.^{23,24}

In equation (9) the inviscid flux variation can be expanded by setting

$$S_{ij} \delta f_j = S_{ij} \frac{\partial f_j}{\partial w} \delta w.$$

Taking the transpose of equation (9), it can be seen that in order to eliminate the explicit dependence on δw in the absence of viscous effect, ψ should be chosen to satisfy the inviscid adjoint equation

$$C_i^T \frac{\partial \psi}{\partial \xi_i} = 0 \quad \text{in } \mathcal{D}, \quad (10)$$

where the inviscid Jacobian matrices in the transformed space are given by

$$C_i = S_{ij} \frac{\partial f_j}{\partial w}.$$

In order to design a shape which will lead to a desired pressure distribution, natural choice is to set

$$I = \frac{1}{2} \int_{\mathcal{B}} (p - p_d)^2 dS$$

where p_d is the desired surface pressure, and the integral is evaluated over the actual surface area. In the computational domain this is transformed to

$$I = \frac{1}{2} \iint_{\mathcal{B}_w} (p - p_d)^2 |S_2| d\xi_1 d\xi_3,$$

where the quantity

$$|S_2| = \sqrt{S_{2j} S_{2j}}$$

denotes the face area corresponding to a unit element of face area in the computational domain. Now, to cancel the dependence of the boundary integral on δp , the adjoint boundary condition reduces to

$$\psi_j n_j = p - p_d \quad (11)$$

where n_j are the components of the surface normal

$$n_j = \frac{S_{2j}}{|S_2|}.$$

This amounts to a transpiration boundary condition on the co-state variables corresponding to the momentum components. Note that it imposes no restriction on the tangential component of ψ at the boundary.

Viscous Adjoint Equations

The viscous terms are derived below under the assumption that the viscosity and heat conduction coefficients μ and k are essentially independent of the flow, and that their variations may be neglected. This simplification has been successfully used for many aerodynamic problems of interest. However, if the flow variations could result in significant changes in the turbulent viscosity, it may be necessary to account for its variation in the calculation.

Transformation to Primitive Variables

The derivation of the viscous adjoint terms can be simplified by transforming to the primitive variables

$$\tilde{w}^T = (\rho, u_1, u_2, u_3, p),$$

because the viscous stresses depend on the velocity derivatives $\frac{\partial u_i}{\partial x_j}$, while the heat flux can be expressed as

$$\kappa \frac{\partial}{\partial x_i} \left(\frac{p}{\rho} \right).$$

where $\kappa = \frac{k}{R} = \frac{\gamma \mu}{Pr(\gamma-1)}$. The relationship between the conservative and primitive variations is defined by the expressions

$$\delta w = M \delta \tilde{w}, \quad \delta \tilde{w} = M^{-1} \delta w$$

which make use of the transformation matrices $M = \frac{\partial w}{\partial \tilde{w}}$ and $M^{-1} = \frac{\partial \tilde{w}}{\partial w}$. These matrices are provided in transposed form for future convenience

$$M^T = \begin{bmatrix} 1 & u_1 & u_2 & u_3 & \frac{u_i u_i}{2} \\ 0 & \rho & 0 & 0 & \rho u_1 \\ 0 & 0 & \rho & 0 & \rho u_2 \\ 0 & 0 & 0 & \rho & \rho u_3 \\ 0 & 0 & 0 & 0 & \frac{1}{\gamma-1} \end{bmatrix}$$

$$M^{-1T} = \begin{bmatrix} 1 & -\frac{u_1}{\rho} & -\frac{u_2}{\rho} & -\frac{u_3}{\rho} & \frac{(\gamma-1)u_i u_i}{2} \\ 0 & \frac{1}{\rho} & 0 & 0 & -(\gamma-1)u_1 \\ 0 & 0 & \frac{1}{\rho} & 0 & -(\gamma-1)u_2 \\ 0 & 0 & 0 & \frac{1}{\rho} & -(\gamma-1)u_3 \\ 0 & 0 & 0 & 0 & \gamma-1 \end{bmatrix}.$$

The conservative and primitive adjoint operators L and \tilde{L} corresponding to the variations δw and $\delta \tilde{w}$ are then related by

$$\int_{\mathcal{D}} \delta w^T L \psi \, d\mathcal{D}_\xi = \int_{\mathcal{D}} \delta \tilde{w}^T \tilde{L} \psi \, d\mathcal{D}_\xi,$$

with

$$\tilde{L} = M^T L,$$

so that after determining the primitive adjoint operator by direct evaluation of the viscous portion of (9), the conservative operator may be obtained by the transformation $L = M^{-1T} \tilde{L}$. Since the continuity equation contains no viscous terms, it makes no

contribution to the viscous adjoint system. Therefore, the derivation proceeds by first examining the adjoint operators arising from the momentum equations and then the energy equation. The details may be found in.²⁵

The Viscous Adjoint Field Operator

In order to make use of the summation convention, it is convenient to set $\psi_{j+1} = \phi_j$ for $j = 1, 2, 3$ and $\psi_5 = \theta$. Collecting together the contributions from the momentum and energy equations, the viscous adjoint operator in primitive variables can be finally expressed as

$$\begin{aligned} (\tilde{L}\psi)_1 &= -\frac{p}{\rho^2} \frac{\partial}{\partial \xi_i} \left(S_{ij} \kappa \frac{\partial \theta}{\partial x_j} \right) \\ (\tilde{L}\psi)_{i+1} &= \frac{\partial}{\partial \xi_i} \left\{ S_{ij} \left[\mu \left(\frac{\partial \phi_i}{\partial x_j} + \frac{\partial \phi_j}{\partial x_i} \right) + \lambda \delta_{ij} \frac{\partial \phi_k}{\partial x_k} \right] \right\} \\ &\quad + \frac{\partial}{\partial \xi_i} \left\{ S_{ij} \left[\mu \left(u_i \frac{\partial \theta}{\partial x_j} + u_j \frac{\partial \theta}{\partial x_i} \right) \lambda \delta_{ij} u_k \frac{\partial \theta}{\partial x_k} \right] \right\} \\ &\quad - \sigma_{ij} S_{lj} \frac{\partial \theta}{\partial \xi_i} \quad \text{for } i = 1, 2, 3 \\ (\tilde{L}\psi)_5 &= \frac{1}{\rho} \frac{\partial}{\partial \xi_i} \left(S_{ij} \kappa \frac{\partial \theta}{\partial x_j} \right). \end{aligned}$$

The conservative viscous adjoint operator may now be obtained by the transformation

$$L = M^{-1T} \tilde{L}.$$

Boundary Conditions for Force Optimization

The boundary term that arises from the momentum equations including both the δw and δS components (9) takes the form

$$\int_{\mathcal{B}} \phi_k \delta (S_{2j} (\delta_{kj} p + \sigma_{kj})) \, d\mathcal{B}_\xi.$$

Replacing the metric term with the corresponding local face area S_2 and unit normal n_j defined by

$$|S_2| = \sqrt{S_{2j} S_{2j}}, \quad n_j = \frac{S_{2j}}{|S_2|}$$

then leads to

$$\int_{\mathcal{B}} \phi_k \delta (|S_2| n_j (\delta_{kj} p + \sigma_{kj})) \, d\mathcal{B}_\xi.$$

Defining the components of the total surface stress as

$$\tau_k = n_j (\delta_{kj} p + \sigma_{kj})$$

and the physical surface element

$$dS = |S_2| \, d\mathcal{B}_\xi,$$

the integral may then be split into two components

$$\int_{\mathcal{B}} \phi_k \tau_k |\delta S_2| \, d\mathcal{B}_\xi + \int_{\mathcal{B}} \phi_k \delta \tau_k \, dS, \quad (12)$$

where only the second term contains variations in the flow variables and must consequently cancel the δw

terms arising in the cost function. The first term will appear in the expression for the gradient.

A general expression for the cost function that allows cancellation with terms containing $\delta\tau_k$ has the form

$$I = \int_{\mathcal{B}} \mathcal{N}(\tau) dS, \quad (13)$$

corresponding to a variation

$$\delta I = \int_{\mathcal{B}} \frac{\partial \mathcal{N}}{\partial \tau_k} \delta \tau_k dS,$$

for which cancellation is achieved by the adjoint boundary condition

$$\phi_k = \frac{\partial \mathcal{N}}{\partial \tau_k}.$$

Natural choices for \mathcal{N} arise from force optimization and as measures of the deviation of the surface stresses from desired target values.

The force in a direction with cosines q_i has the form

$$C_q = \int_{\mathcal{B}} q_i \tau_i dS.$$

If we take this as the cost function (13), this quantity gives

$$\mathcal{N} = q_i \tau_i.$$

Cancellation with the flow variation terms in equation (12) therefore mandates the adjoint boundary condition

$$\phi_k = q_k.$$

Note that this choice of boundary condition also eliminates the first term in equation (12) so that it need not be included in the gradient calculation.

Inverse Design

In the inverse design case, where the cost function is intended to measure the deviation of the surface stresses from some desired target values, a suitable definition is

$$\mathcal{N}(\tau) = \frac{1}{2} a_{lk} (\tau_l - \tau_{dl}) (\tau_k - \tau_{dk}),$$

where τ_d is the desired surface stress, including the contribution of the pressure, and the coefficients a_{lk} define a weighting matrix. For cancellation

$$\phi_k \delta \tau_k = a_{lk} (\tau_l - \tau_{dl}) \delta \tau_k.$$

This is satisfied by the boundary condition

$$\phi_k = a_{lk} (\tau_l - \tau_{dl}). \quad (14)$$

Assuming arbitrary variations in $\delta\tau_k$, this condition is also necessary.

In order to control the surface pressure and normal stress one can measure the difference

$$n_j \{ \sigma_{kj} + \delta_{kj} (p - p_d) \},$$

where p_d is the desired pressure. The normal component is then

$$\tau_n = n_k n_j \sigma_{kj} + p - p_d,$$

so that the measure becomes

$$\begin{aligned} \mathcal{N}(\tau) &= \frac{1}{2} \tau_n^2 \\ &= \frac{1}{2} n_l n_m n_k n_j \{ \sigma_{lm} + \delta_{lm} (p - p_d) \} \\ &\quad * \{ \sigma_{kj} + \delta_{kj} (p - p_d) \}. \end{aligned}$$

This corresponds to setting

$$a_{lk} = n_l n_k$$

in equation (14). Defining the viscous normal stress as

$$\tau_{vn} = n_k n_j \sigma_{kj},$$

the measure can be expanded as

$$\begin{aligned} \mathcal{N}(\tau) &= \frac{1}{2} n_l n_m n_k n_j \sigma_{lm} \sigma_{kj} \\ &\quad + \frac{1}{2} (n_k n_j \sigma_{kj} + n_l n_m \sigma_{lm}) (p - p_d) \\ &\quad + \frac{1}{2} (p - p_d)^2 \\ &= \frac{1}{2} \tau_{vn}^2 + \tau_{vn} (p - p_d) + \frac{1}{2} (p - p_d)^2. \end{aligned}$$

For cancellation of the boundary terms

$$\begin{aligned} \phi_k (n_j \delta \sigma_{kj} + n_k \delta p) &= \{ n_l n_m \sigma_{lm} + n_l^2 (p - p_d) \} n_k \\ &\quad * (n_j \delta \sigma_{kj} + n_k \delta p) \end{aligned}$$

leading to the boundary condition

$$\phi_k = n_k (\tau_{vn} + p - p_d).$$

In the case of high Reynolds number, this is well approximated by the equations

$$\phi_k = n_k (p - p_d), \quad (15)$$

which should be compared with the single scalar equation derived for the inviscid boundary condition (11). In the case of an inviscid flow, choosing

$$\mathcal{N}(\tau) = \frac{1}{2} (p - p_d)^2$$

requires

$$\phi_k n_k \delta p = (p - p_d) n_k^2 \delta p = (p - p_d) \delta p$$

which is satisfied by equation (15), but which represents an over-specification of the boundary condition since only the single condition (11) needs be specified to ensure cancellation.

Boundary Conditions Arising from the Energy Equation

The form of the boundary terms arising from the energy equation depends on the choice of temperature boundary condition at the wall. For the adiabatic case, the boundary contribution is

$$\int_{\mathcal{B}} k\delta T \frac{\partial \theta}{\partial n} d\mathcal{B}_{\xi},$$

while for the constant temperature case the boundary term is

$$\int_{\mathcal{B}} k\theta \left\{ \frac{S_{2j}^2}{J} \frac{\partial}{\partial \xi_2} \delta T + \delta \left(\frac{S_{2j}^2}{J} \right) \frac{\partial T}{\partial \xi_2} \right\} d\mathcal{B}_{\xi}.$$

one possibility is to introduce a contribution into the cost function which depends on T or $\frac{\partial T}{\partial n}$ so that the appropriate cancellation would occur. Since there is little physical intuition to guide the choice of such a cost function for aerodynamic design, a more natural solution is to set

$$\theta = 0$$

in the constant temperature case or

$$\frac{\partial \theta}{\partial n} = 0$$

in the adiabatic case. Note that in the constant temperature case, this choice of θ on the boundary would also eliminate the boundary metric variation terms in

$$\int_{\mathcal{B}} \theta \delta (S_{2j} Q_j) d\mathcal{B}_{\xi}.$$

IMPLEMENTATION

Cost Function for Planform Design

In order to design a high performance transonic wing, which will lead to a desired pressure distribution, and to still maintain a realistic shape, the natural choice is to set

$$I = \alpha_1 C_D + \alpha_2 \frac{1}{2} \int_{\mathcal{B}} (p - p_d)^2 dS + \alpha_3 C_W \quad (16)$$

with

$$C_W = \frac{\mathcal{W}_{wing}}{q_{\infty} S_{ref}} \quad (17)$$

where

C_D	=	drag coefficient,
C_W	=	dimensionless wing structural weight,
p	=	current surface pressure,
p_d	=	desired pressure,
q_{∞}	=	dynamic pressure,
S_{ref}	=	reference area,
\mathcal{W}_{wing}	=	wing structure weight, and
$\alpha_1, \alpha_2, \alpha_3$	=	weighting parameter for drag, inverse design, and structural weight respectively.

The constant α_2 is introduced to provide the designer some control over the pressure distribution.

A practical way to estimate \mathcal{W}_{wing} is to use the so-called Statistical Group Weights Method, which applies statistical equations based on sophisticated regression analysis. For a cargo/transport wing weight, one can use²⁶

$$\mathcal{W}_{weight} = 0.0051 (W_{dg} N_z)^{0.557} S_w^{0.649} A^{0.5} (t/c)_{root}^{-0.4} (1 + \lambda)^{0.1} \cos(\Lambda)^{-1.0} S_{csw}^{0.1} \quad (18)$$

where

A	=	aspect ratio,
N_z	=	ultimate load factor = 1.5 x limit load factor,
S_{csw}	=	control surface area (wing-mounted),
S_w	=	trapezoidal wing area,
t/c	=	thickness to chord ratio,
W_{dg}	=	flight design gross weight,
Λ	=	wing sweep, and
λ	=	taper ratio at 25 % MAC.

In addition, if the wing of interest is modeled by five planform variables such as root chord (c_1), mid-span chord (c_2), tip chord (c_3), span (b), and sweepback (Λ), as shown in Fig. 1, the sensitivity of the weight to an individual planform variable can be shown in Fig. 2, indicating that the weight increases, as sweepback, span, or chord-length increases.

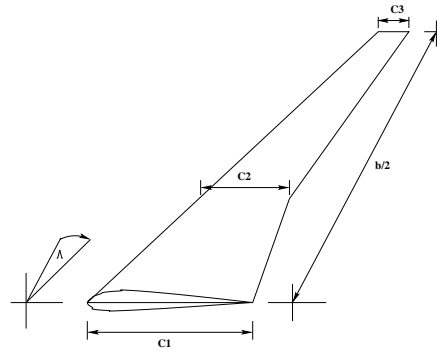


Fig. 1 Modeled wing governed by five planform variables; root chord (c_1), mid-span chord (c_2), tip chord (c_3), span (b), and sweepback (Λ).

The increases of sweepback, span, and chord-length affect drag oppositely. As sweepback is increased, the shock drag is weakened. Vortex drag can be reduced by increasing the span.

In these ways the inclusion of a weight estimate in the cost function should prevent the optimization from leading to an unrealistic wing planform, and yield a good overall performance.

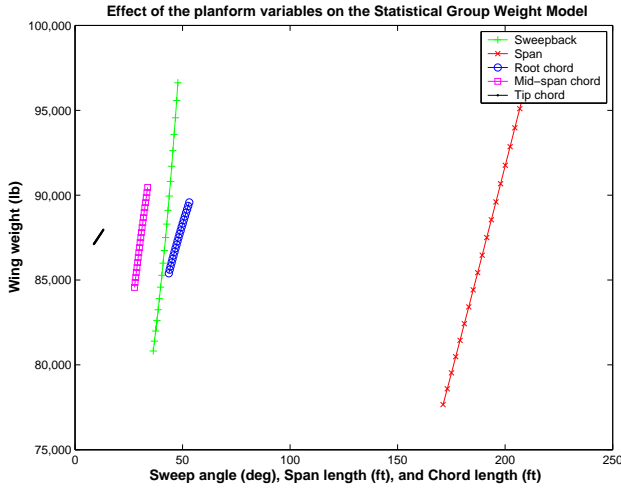


Fig. 2 Effect of sweepback(Λ), span (b), root chord(c_1), mid-span chord(c_2), and tip chord(c_3) on the Statistical Group Weights Method

Aerodynamic Gradient Calculation for Planform Variables

Gradient information can be computed using a variety of approaches such as the finite-difference method, the complex step method,¹² and the automatic differentiation.¹³ Unfortunately, their computational cost is still proportional to the number of design variables in the problem. In an optimum transonic wing design, suppose one chooses mesh points on a wing surface as the design variables, which is on the order of 1000 or more; it is impractical to calculate the gradient using the methods mentioned earlier. In our planform optimization, the design variables are points on the wing surface plus the planform variables. To evaluate the aerodynamic gradient with respect to the planform variables, since the number of planform variables (five in this study) is far less than that of the surface optimization, one could calculate the gradient by the finite-difference method, the complex step method or the automatic differentiation. However, the cost for the gradient calculation will be five times higher. A more efficient approach is to follow the adjoint formulation.

Consider the aerodynamic contribution of the cost function (16)

$$\delta I = \int_{\mathcal{B}} \delta \mathcal{M} d\mathcal{B}_{\xi} + \int_{\mathcal{D}} \psi^T \delta R d\mathcal{D}_{\xi}$$

This can be split as

$$\delta I = [I_w]_I \delta w + \delta I_{II}$$

with

$$\delta \mathcal{M} = [\mathcal{M}_w]_I \delta w + \delta \mathcal{M}_{II}$$

where the subscripts I and II are used to distinguish between the contributions associated with variation of

the flow solution δw and those associated with the metric variations δS . Thus $[\mathcal{M}_w]_I$ represents $\frac{\partial \mathcal{M}}{\partial w}$ with the metrics fixed. Note that δR is intentionally kept unsplit for programming purposes. If one chooses ψ as ψ^* that satisfy the adjoint equations, then

$$\begin{aligned} \delta I(w, S) &= \delta I(S) \\ &= \int_{\mathcal{B}} \delta \mathcal{M}_{II} d\mathcal{B}_{\xi} + \int_{\mathcal{D}} \psi^{*T} \delta R d\mathcal{D}_{\xi} \\ &\approx \sum_{\mathcal{B}} \delta \mathcal{M}_{II} \Delta \mathcal{B} + \sum_{\mathcal{D}} \psi^{*T} \Delta \bar{R} \\ &\approx \sum_{\mathcal{B}} \delta \mathcal{M}_{II} \Delta \mathcal{B} + \sum_{\mathcal{D}} \psi^{*T} (\bar{R}|_{S+\delta S} - \bar{R}|_S), \end{aligned}$$

where $\bar{R}|_S$ and $\bar{R}|_{S+\delta S}$ are volume weighted residuals calculated at the original mesh and at the mesh perturbed in the design direction.

Provided that ψ^* has already been calculated and \bar{R} can be easily calculated, the gradient of the planform variables can be computed effectively by first perturbing all the mesh points along the direction of interest. For example, to calculate the gradient with respect to the sweepback, move all the points on the wing surface as if the wing were pushed backward and also move all other associated points in the computational domain to match the new location of points on the wing. Then re-calculate the residual value and subtract the previous residual value from the new value to form $\Delta \bar{R}$. Finally, to calculate the planform gradient, multiply $\Delta \bar{R}$ by the costate vector and add the contribution from the boundary terms.

This way of calculating the planform gradient exploits the full benefit of knowing the value of adjoint variables ψ^* with no extra cost of flow or adjoint calculations.

Choice of Weighting Constants

Performance Consideration

The choice of α_1 and α_3 greatly affects the optimum shape. An intuitive choice of α_1 and α_3 can be made by considering the problem of maximizing range of an aircraft. The simplified range equation can be expressed as

$$R = \frac{V L}{C D} \log \frac{W_1}{W_2}$$

where

- C = Specific Fuel Consumption,
- D = Drag,
- L = Lift,
- R = Range,
- V = Aircraft velocity,
- W_1 = Take off weight, and
- W_2 = Landing weight.

If one takes

$$W_1 = W_e + W_f = \text{fixed}$$

$$W_2 = W_e$$

where

W_e = Gross weight of the airplane without fuel,

W_f = Fuel weight,

then the variation of the weight can be expressed as

$$\delta W_2 = \delta W_e \approx \delta W_{wing}.$$

With fixed $\frac{V}{C}$, W_1 , and L , the variation of R can be stated as

$$\begin{aligned} \delta R &= \frac{V}{C} \left(\delta \left(\frac{L}{D} \right) \log \frac{W_1}{W_2} + \frac{L}{D} \delta \left(\log \frac{W_1}{W_2} \right) \right) \\ &= \frac{V}{C} \left(-\frac{\delta D}{D} \frac{L}{D} \log \frac{W_1}{W_2} - \frac{L}{D} \frac{\delta W_2}{W_2} \right) \\ &= -\frac{V L}{C D} \log \frac{W_1}{W_2} \left(\frac{\delta D}{D} + \frac{1}{\log \frac{W_1}{W_2}} \frac{\delta W_2}{W_2} \right) \end{aligned}$$

and

$$\begin{aligned} \frac{\delta R}{R} &= - \left(\frac{\delta C_D}{C_D} + \frac{1}{\log \frac{W_1}{W_2}} \frac{\delta W_2}{W_2} \right) \\ &= - \left(\frac{\delta C_D}{C_D} + \frac{1}{\log \frac{W_1}{W_2} \frac{W_2}{q_\infty S_{ref}}} \frac{\delta C_W}{W_2} \right). \end{aligned}$$

If we minimize the cost function defined as

$$I = C_D + \alpha C_W,$$

where α is the weighting multiplication, then choosing

$$\alpha = \frac{C_D}{\frac{W_2}{q_\infty S_{ref}} \log \frac{W_1}{W_2}}, \quad (19)$$

corresponds to maximizing the range of the aircraft.

Application of Game Theory

To extend the optimal design range, $\frac{\alpha_3}{\alpha_1}$ should not be limited to only one value. Using different values of $\frac{\alpha_3}{\alpha_1}$, different optimal shapes can be created. If the optimal shapes are truly optimized, each of them should lie on a curve where no improvement can be achieved in drag that doesn't lead to a degradation of weight, and the similar. This idea is similar to a "game" where one player tries to minimize C_D and the other player tries to minimize C_W .

We use an array of different (α_1, α_3) to compute different optimum shapes. Then, we eliminate any dominated shape to form an optimal set, the "Pareto front". For example, suppose Fig. 3 represents a result of optimum shapes corresponding to an array of different (α_1, α_3) . Let the symbol X represent one optimum shape. In this example, the point Q is dominated by the point P (same drag, less weight) and also by the point R (less drag, same weight). So the point Q will be eliminated. The Pareto front can be fit through the points P, R, and other dominating points and eliminating all the other dominated points illustrated in the figure. With the Pareto front representation, the designer will have freedom to pick the most useful optimal design.

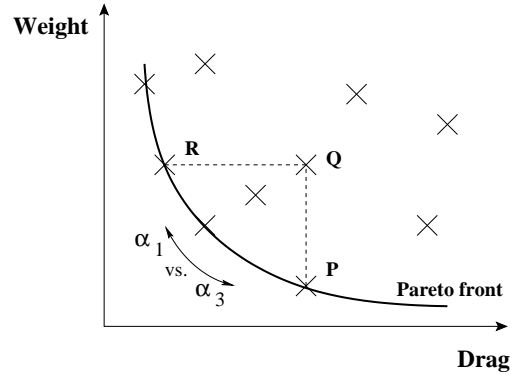


Fig. 3 Cooperative game strategy with Drag and Weight as players

DESIGN CYCLE AND PARALLEL COMPUTATION

In general, the computational cost of viscous design is at least one order of magnitude greater than the cost of inviscid design. Three main reasons for this are the increase of the number of grid points by a factor of two or more to resolve the boundary layer, the additional cost of computing the viscous terms and turbulent model, and a slower convergence due to highly stretched cells inside the boundary layers.

To make the design method feasible in practice, parallel computing is implemented to parts of the design cycle that dominate the computation time. Both flow and adjoint calculation have been implemented in a parallel setting using the message passing interface (MPI).

The design cycle starts by first solving the flow field until about a 3 order of magnitude drop in the residual. The flow solution is then passed to the adjoint solver. Second, the adjoint solver is run to calculate the costate vector. Iteration continues until at least a 2 order of magnitude drop in the residual.¹ The costate vector is passed to the gradient module to evaluate the aerodynamic gradient. Then, the structural gradient is calculated and added to the aerodynamic gradient to form the overall gradient. The steepest descent method is used with a small step size to guarantee that the solution will converge to the optimum point. The design cycle is shown in Fig. 4.

FLOW SOLVER AND ADJOINT SOLVER

The flow solver and the adjoint solver chosen in this work are codes developed by Jameson.^{21, 28-30} The flow solver solves the three dimensional Navier-Stokes equations by employing the JST scheme, together with a multistage explicit time stepping scheme. Rapid convergence to a steady state is achieved via variable local time steps, residual averaging, and a full approximation multi-grid scheme. The adjoint solver solves

¹Studies²⁷ have shown that, for the design purpose, only a 3 order of magnitude drop in the residual of the flow calculation and only a 2 order of magnitude drop in the residual of the adjoint calculation are sufficient.

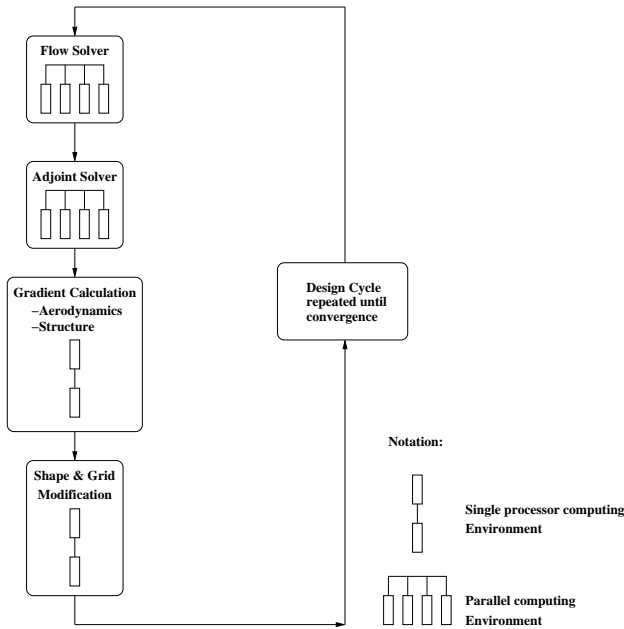


Fig. 4 Design cycle

the corresponding adjoint equations using similar techniques to those of the flow solver. In fact much of the software is shared by the flow and adjoint solvers.

RESULTS

Redesign of Boeing 747 wing

We present results to show that the optimization can successfully trade planform parameters. In these calculations the flow was modeled by the Reynolds Averaged Navier-Stokes equation, with a Baldwin Lomax turbulence model. This turbulence model was considered sufficient because the optimization is near the cruise condition with attach flow. The case chosen is the Boeing 747 wing fuselage combination at Mach 0.90 and a lift coefficient $C_L = 0.42$. The computational mesh is shown in Fig. 5.

In this test case, the Mach Number is significantly higher than the current normal cruising Mach number of 0.85. We allowed section changes together with variations of sweepback, span, root chord, mid-span chord, and tip chord. Figure 6 shows a baseline calculation with the planform fixed. Here the drag was reduced from 181.9 counts to 127.9 counts (29.7% reduction) in 50 design iterations with relatively small changes in the section shape.

Figure 7 shows the effect of allowing changes in sweepback, span, root chord, mid-span chord, and tip chord. The parameter α_3 was chosen according to formula (19) such that the cost function corresponds to maximizing the range of the aircraft. In 50 design iterations the drag was reduced from 181.9 counts to 124.9 counts (31.3% reduction), while the dimensionless structure weight was slightly increased from 0.02956 to .03047 (3.1% increase). This test case shows a good trade off among the planform variables to

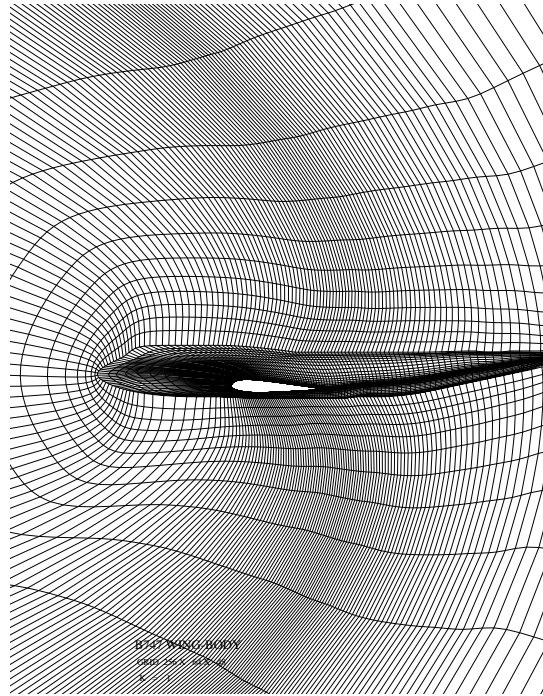


Fig. 5 Computational Grid of the B747-200 Wing Fuselage

achieve an optimal performance for a realistic design. At Mach 0.9, which is an off design point, drag is quite high. As a result, the optimizer increases the sweepback to weaken shock drag, increases the length of the span to reduce vortex drag, and reduces thickness to chord ratio (with the thickness fixed) to alleviate shock drag. However, these changes cause a slight increase of wing weight. But if the wing structural weight is not included in the cost function, the optimal shape will result in an excessive span, chord-length, and sweep angle.

As a result of the trade between drag reductions due to the increase in sweepback and span, and increased wing weight, the overall drag reduction was more than in the previous figure, while the wing weight was slightly increased. These results verify the feasibility of including the effects of planform variations in the optimization.

Pareto Front

The problem of optimizing both drag and weight can be treated as a multi-objective function optimization. However, the multiple objective functions can be combined to a single objective function using weighting constants, as done in this paper. A different choice of α_1 and α_3 will result in a different optimum shape. The optimum shapes should not dominate each other, and therefore lie on the Pareto front, where no improvement can be achieved in one objective component that doesn't lead to degradation in the remaining component. Therefore, by varying α_1 and α_3 , it is possible to compute the Pareto front.

Figure 8 shows the effect of the weighting parameters (α_1, α_3) on the optimal design. As before the design variables are sweepback, span, chords at three different span locations and mesh points on the wing surface. In Fig. 8 each point corresponds to an optimal shape for one specific choice of (α_1, α_3). By varying α_1 and α_3 , we capture a Pareto front that bounds all the solutions. All points on this front are acceptable solutions, and any further choice to select the final design depends on the nature of the problem and several other factors. The Pareto front can be very useful to the designer because it represents a set which is optimal in the sense that no improvement can be achieved in one objective component that doesn't lead to degradation in at least one of the remaining components. The optimum shape that corresponds to the optimal Breguet range is also marked in the figure.

Figure 9 shows the change of planform when the ratio $\frac{\alpha_3}{\alpha_1} = 1$. This ratio of $\frac{\alpha_3}{\alpha_1}$ is sufficient to cause the optimizer to reduce the sweepback, reducing wing weight. But it allows the optimizer to increase the span, reducing vortex drag. This yields an optimum shape which has low structure weight and moderate drag.

CONCLUSION

The shape changes in the section needed to improve the transonic wing design are quite small. However, in order to obtain a true optimum design larger scale changes such as changes in the wing planform (sweepback, span, chord, and taper) should be considered. Because these directly affect the structure weight, a meaningful result can only be obtained by considering a cost function that takes account of both the aerodynamic characteristics and the weight.

This paper develops and validates an aerodynamic design methodology based on the Navier-Stokes equations for planform optimization. A model for the structural weight is included in the design cost function. The results of optimizing a wing-fuselage of a commercial transonic transport aircraft has highlighted the importance of the structural weight model and the viscous effects on the design process. The trade-off between the structural cost function and the aerodynamic cost function prevents an unrealistic result and leads to a useful design. The inclusion of viscous effects increases the level of realism of the design. Methods of combining drag and wing weight also provide the designer a better opportunity to choose the final optimum shape.

ACKNOWLEDGMENT

This work has benefited greatly from the support of the Air Force Office of Science Research under grant No. AF F49620-98-1-2002.

References

¹F. Bauer, P. Garabedian, D. Korn, and A. Jameson. *Supercritical Wing Sections II*. Springer Verlag, New York, 1975.

²P. R. Garabedian and D. G. Korn. Numerical design of transonic airfoils. In B. Hubbard, editor, *Proceedings of SYNSPADE 1970*, pages 253–271, Academic Press, New York, 1971.

³R. M. Hicks and P. A. Henne. Wing design by numerical optimization. *Journal of Aircraft*, 15:407–412, 1978.

⁴J. Fay. *On the Design of Airfoils in Transonic Flow Using the Euler Equations*. Ph.D. Dissertation, Princeton University 1683-T, 1985.

⁵R. Campbell. An approach to constrained aerodynamic design with application to airfoils. *NASA Technical Paper 3260*, Langley Research Center, November 1992.

⁶A. Jameson. Aerodynamic design via control theory. *Journal of Scientific Computing*, 3:233–260, 1988.

⁷A. Jameson. Optimum aerodynamic design using CFD and control theory. *AIAA paper 95-1729*, AIAA 12th Computational Fluid Dynamics Conference, San Diego, CA, June 1995.

⁸J. Reuther, A. Jameson, J. Farmer, L. Martinelli, and D. Saunders. Aerodynamic shape optimization of complex aircraft configurations via an adjoint formulation. *AIAA paper 96-0094*, 34th Aerospace Sciences Meeting and Exhibit, Reno, Nevada, January 1996.

⁹J. Reuther, J. J. Alonso, J. C. Vassberg, A. Jameson, and L. Martinelli. An efficient multiblock method for aerodynamic analysis and design on distributed memory systems. *AIAA paper 97-1893*, June 1997.

¹⁰J. J. Reuther, A. Jameson, J. J. Alonso, M. Rimlinger, and D. Saunders. Constrained multipoint aerodynamic shape optimization using an adjoint formulation and parallel computers: Part I. *Journal of Aircraft*, 36(1):51–60, 1999.

¹¹J. J. Reuther, A. Jameson, J. J. Alonso, M. Rimlinger, and D. Saunders. Constrained multipoint aerodynamic shape optimization using an adjoint formulation and parallel computers: Part II. *Journal of Aircraft*, 36(1):61–74, 1999.

¹²J. R. R. A. Martins, I. M. Kroo, and J. J. Alonso. An automated method for sensitivity analysis using complex variables. *AIAA paper 2000-0689*, 38th Aerospace Sciences Meeting, Reno, Nevada, January 2000.

¹³C. Bischof, A. Carle, G. Corliss, A. Griewank, and P. Hovland. Generating derivative codes from Fortran programs. *Internal report MCS-P263-0991*, Computer Science Division, Argonne National Laboratory and Center of Research on Parallel Computation, Rice University, 1991.

¹⁴J.L. Lions. *Optimal Control of Systems Governed by Partial Differential Equations*. Springer-Verlag, New York, 1971. Translated by S.K. Mitter.

¹⁵O. Pironneau. *Optimal Shape Design for Elliptic Systems*. Springer-Verlag, New York, 1984.

¹⁶A. Jameson. Re-engineering the design process through computation. *AIAA paper 97-0641*, 35th Aerospace Sciences Meeting and Exhibit, Reno, Nevada, January 1997.

¹⁷J. Reuther, J.J. Alonso, M.J. Rimlinger, and A. Jameson. Aerodynamic shape optimization of supersonic aircraft configurations via an adjoint formulation on parallel computers. *AIAA paper 96-4045*, 6th AIAA/NASA/ISSMO Symposium on Multidisciplinary Analysis and Optimization, Bellevue, WA, September 1996.

¹⁸O. Baysal and M. E. Eleshaky. Aerodynamic design optimization using sensitivity analysis and computational fluid dynamics. *AIAA paper 91-0471*, 29th Aerospace Sciences Meeting, Reno, Nevada, January 1991.

¹⁹W. K. Anderson and V. Venkatakrishnan. Aerodynamic design optimization on unstructured grids with a continuous adjoint formulation. *AIAA paper 97-0643*, 35th Aerospace Sciences Meeting and Exhibit, Reno, Nevada, January 1997.

²⁰A. Jameson and L. Martinelli. Aerodynamic shape optimization techniques based on control theory. Technical report, CIME (International Mathematical Summer Center), Martina Franca, Italy, 1999.

²¹A. Jameson. A perspective on computational algorithms for aerodynamic analysis and design. *Progress in Aerospace Sciences*, 37:197–243, 2001.

²²K. Leoviriyakit and A. Jameson. Aerodynamic shape optimization of wings including planform variables. *AIAA paper 2003-0210*, 41st Aerospace Sciences Meeting & Exhibit, Reno, Nevada, January 2003.

²³A. Jameson. Automatic design of transonic airfoils to reduce the shock induced pressure drag. In *Proceedings of the 31st Israel Annual Conference on Aviation and Aeronautics, Tel Aviv*, pages 5–17, February 1990.

²⁴A. Jameson. Optimum aerodynamic design using control theory. *Computational Fluid Dynamics Review*, pages 495–528, 1995.

²⁵A. Jameson. Aerodynamic shape optimization using the adjoint method. 2002-2003 lecture series at the von karman institute, Von Karman Institute For Fluid Dynamics, Brussels, Belgium, February 3-7 2003.

²⁶Daniel P. Raymer. *Aircraft Design: A Conceptual Approach, Third Edition*. AIAA Education Series, Wright-Patterson Air Force Base, Ohio, 1990.

²⁷S. Kim, J. J. Alonso, and A. Jameson. A gradient accuracy study for the adjoint-based navier-stokes design method. *AIAA paper 99-0299*, AIAA 37th Aerospace Sciences Meeting & Exhibit, Reno, NV, January 1999.

²⁸A. Jameson, L. Martinelli, and N. A. Pierce. Optimum aerodynamic design using the Navier-Stokes equations. *Theoretical and Computational Fluid Dynamics*, 10:213–237, 1998.

²⁹A. Jameson. Analysis and design of numerical schemes for gas dynamics 1, artificial diffusion, upwind biasing, limiters and their effect on multigrid convergence. *Int. J. of Comp. Fluid Dyn.*, 4:171–218, 1995.

³⁰A. Jameson. Analysis and design of numerical schemes for gas dynamics 2, artificial diffusion and discrete shock structure. *Int. J. of Comp. Fluid Dyn.*, 5:1–38, 1995.

Mach: 0.900 Alpha: 1.765
 CL: 0.419 CD: 0.01279 CM:-0.1384
 Design: 50 Residual: 0.3633E+00
 Grid: 257X 65X 49
 Sweep: 42.1138 Span(ft): 212.43
 C1(ft): 48.13 C2: 29.13 C3: 10.78
 CW: 0.02956 I: 0.01279

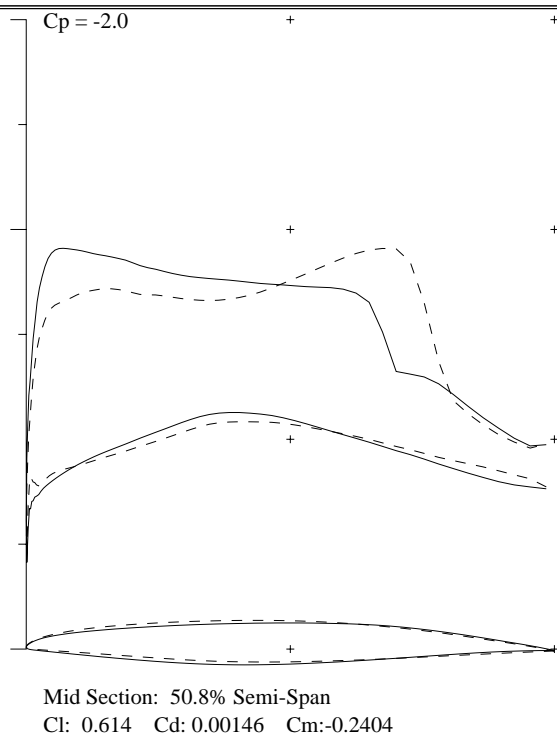
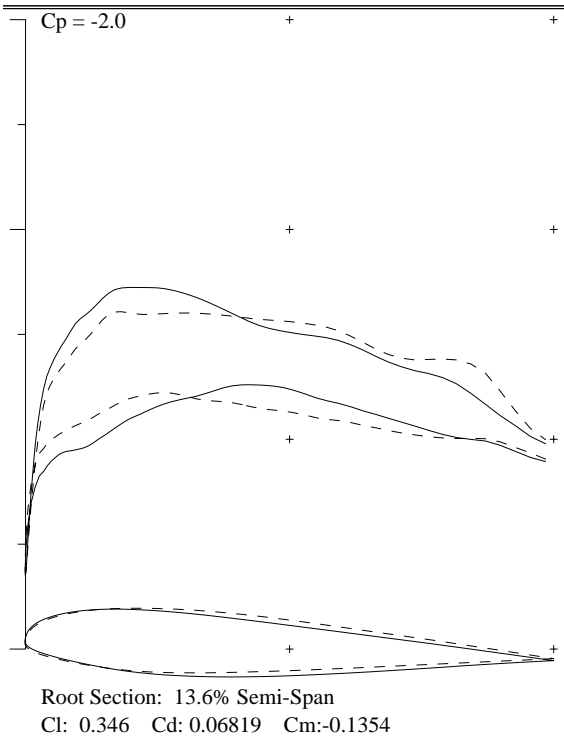
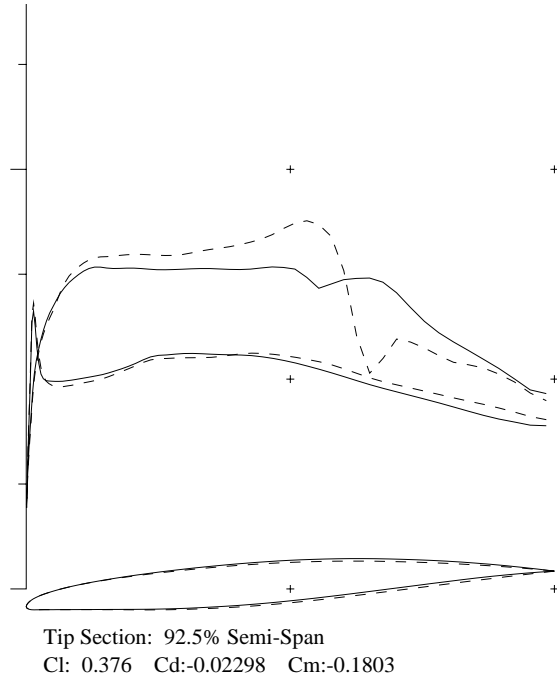
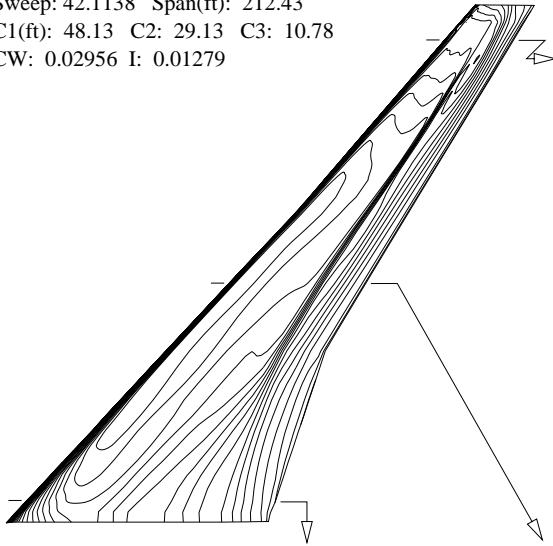


Fig. 6 Redesign of Boeing 747, fixed platform

Mach: 0.900 Alpha: 1.760
 CL: 0.419 CD: 0.01249 CM:-0.1612
 Design: 50 Residual: 0.4527E+00
 Grid: 257X 65X 49
 Sweep: 43.0188 Span(ft): 213.48
 C1(ft): 48.48 C2: 29.99 C3: 11.15
 CW: 0.03047 I: 0.02163

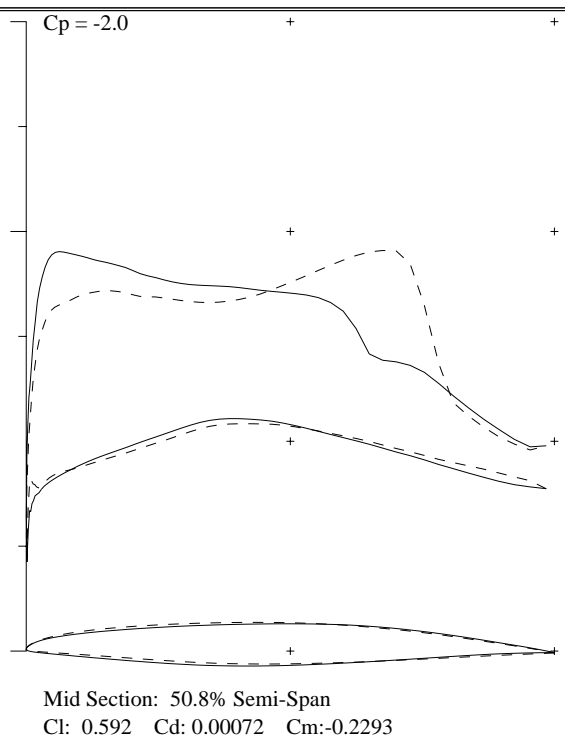
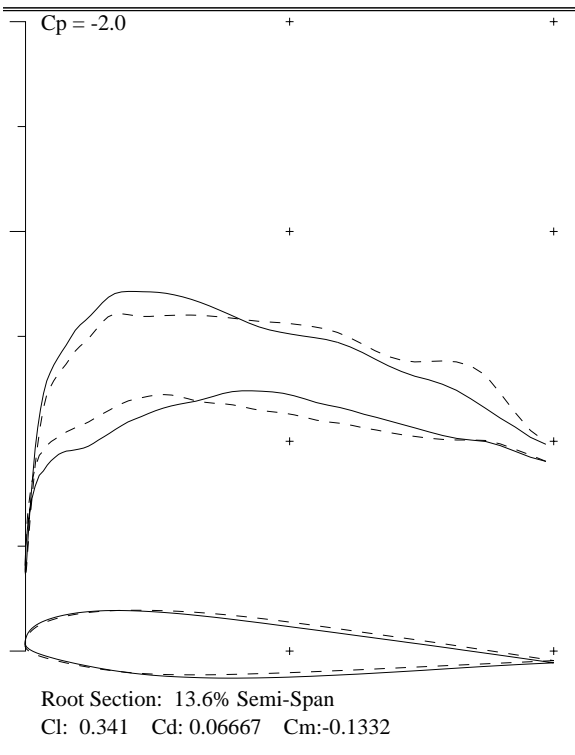
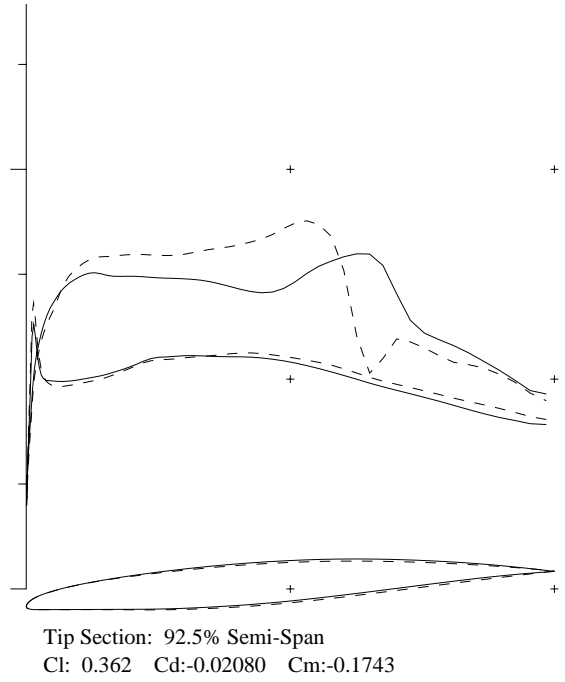
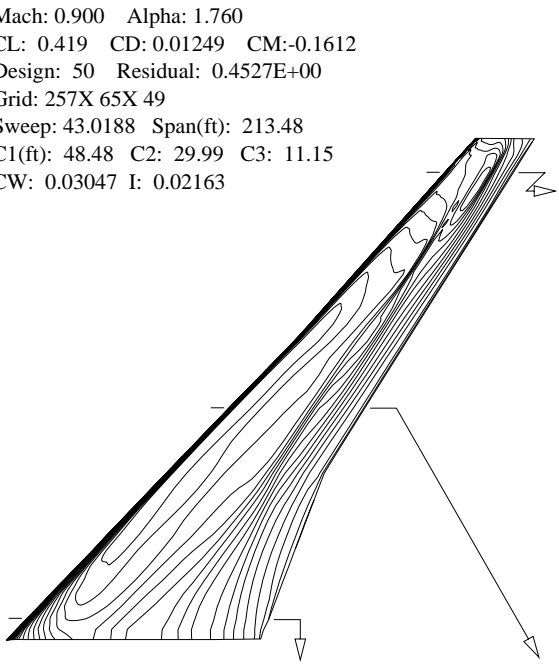


Fig. 7 Redesign of Boeing 747, variable planform and maximizing range

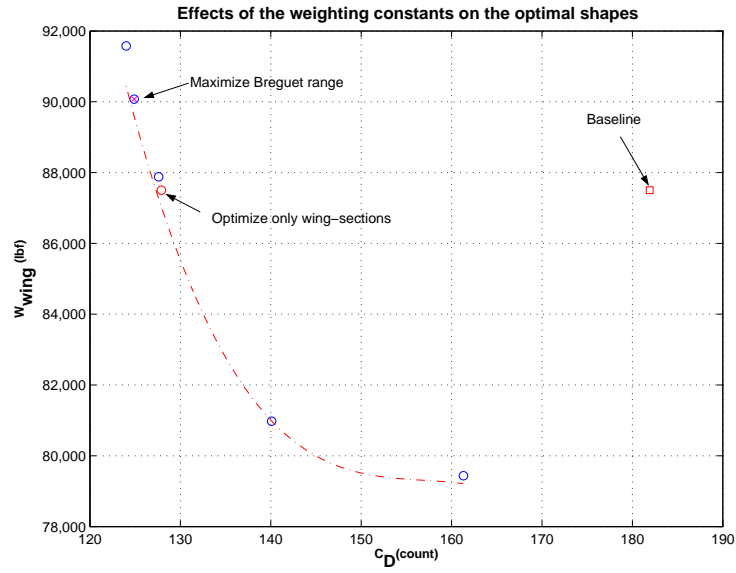


Fig. 8 Pareto front of section and planform modifications

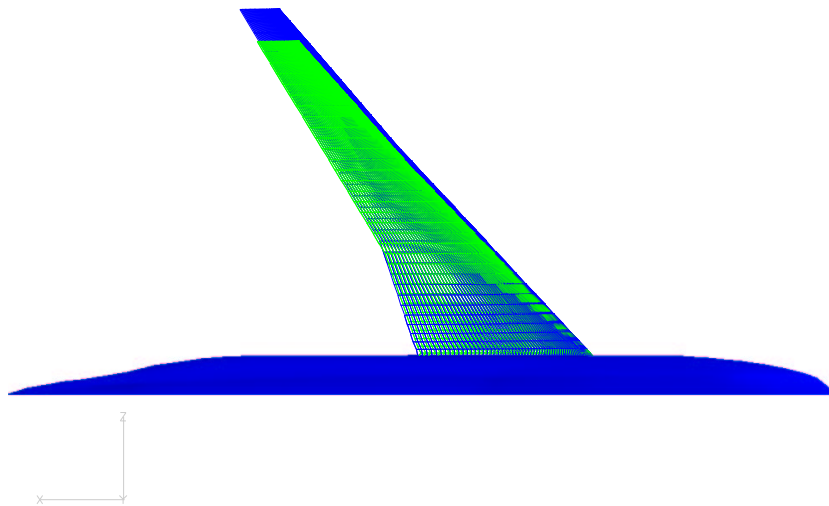


Fig. 9 Superposition of the baseline geometry (green/light) and the optimized planform geometry (blue/dark), using $\alpha_1=1$ and $\alpha_3=1$